

HIGH-PERFORMANCE EPOXY HYBRID NANOCOMPOSITES MODIFIED BY NANOCCLAY AND PES

B. Zhang, Y. Wang*

Department of Polymer and Composite Materials, Beihang University, Beijing, China

* Corresponding author (stevenwangst@hotmail.com)

Keywords: *nanocomposite, fracture toughness, organoclay, PES, epoxy*

1 Introduction

Epoxy resins are widely used as the matrix of fiber reinforced polymer (FRP) composites^[1]. However, their major drawback is that they are too brittle to be used in some circumstances. Since 1980s, great efforts have been made to make up for this demerit and lots of research on the morphologies of these polymer blends and composites was conducted^[2-4]. The addition of rubbery into the epoxy resins markedly improved the toughness of epoxy resins, while it led to the decrease in the elastic modulus and service temperature of epoxy resins. In the following, high performance engineering thermoplastics such as polyethersulphone(PES), polyetherimide(PEI), poly(methyl methacrylate)(PMMA) and polyetheretherketone(PEEK) were used to toughen epoxy resins because of their good toughness, high modulus and high glass transition temperature. Usually, the incorporated phase can separate from the epoxy matrix to form a two-phase structure during the curing reaction and formation of co-continuous phase structure can give rise to the maximal toughness in these blends. However, high content of thermoplastic is commonly needed for the formation of bicontinuous phase structure. Accordingly, it will lead to the increase in viscosity of the reaction mixtures and make the thermoplastic/epoxy blends hard to process. Moreover, the lower T_g formed by phase separation similar to that of the pure epoxy resins lowers the service temperature of the polymer blends. As a result, homogeneous thermoplastic-modified epoxy resins were prepared to solve the disturbing headache. The homogeneous polymer blends with semi-interpenetrating polymer network (semi-IPN) can acquire higher fracture toughness with the incorporation of low content of thermoplastics.

At the same time, inorganic rigid particles were quite popular to toughen polymers. As inorganic rigid particles, montmorillonite and glass bead were widely used to toughen epoxy resins and significantly improved their thermal performances and mechanical properties simultaneously. Since 1990s, nanotechnology has been developing very rapidly and the incorporation of nanoparticles, especially nanomontmorillonite, into the epoxy matrix has been seen as one of promising ways to toughen the epoxy resins. According to the references, these nanoparticles enhanced the stiffness, the toughness and thermal performances of the materials at the same time. Moreover, their morphology and dispersion in the epoxy matrix are critical to the ultimate properties of the nanocomposites.

In recent years, the incorporation of two phases into the epoxy matrix to attain synergy of toughening has drawn more and more attention^[5-8]. However, the toughening mechanism of two-toughener system is more complicated and the synergy of the two toughening components is hard to take place. As a result, further research should be done on this aspect.

In this research, we aim to use organoclay to supplementarily toughen PES/epoxy blends and acquire organoclay/PES/epoxy hybrid nanocomposites with homogenous matrices. We also try to find the toughening mechanism in the hybrid nanocomposite system.

2 Experimental

2.1 Materials

The epoxy resin used in this investigation is DER331[®], the diglycidyl ether of bisphenol-A (DGEBA), provided by Dow Chemical Company. The epoxy equivalent weight is 182-192g/eq. The hardener is 4,4'-diaminodiphenyl

sulphone (DDS), acquired from SUZHOU YINSHENG chemiacal Co.,Ltd. Polythiersulphone (PES) is an amorphous thermoplastic, supplied by Sumitomo Corporation as a toughener. Octadecylamine modified montmorillonite named I. 30E was purchased from Nanocor, Inc. as another toughener. Methylene chloride was used as the solvent, produced by Tianjin Kermel Chemical Reagent Co., Ltd. The release agent is Frekote 44-NC, obtained from Loctite Corporation. All the chemicals and resins were used as received.

2.2 Preparation of samples

2.2.1 Preparation of hybrid nanocomposites

PES, organoclay and DDS were desiccated in vacuum for more than 48h at 80 °C before experiments. PES (5wt%) was weighted and completely dissolved in methylene chloride at room temperature.. Then epoxy oligomer was incorporated to the solution and dissolved in it. In the following, organoclay (1wt% and 3wt%, respectively) was weighed and dispersed in the solution with vigorous mechanical stir. In the next step, high Shear-resistant emulsion equipment was used to further disperse the organoclay at 10000rpm for more than 30min, followed by sonication for at least 30 min. The translucent mixture was heated to 80°C in a water bath to drive off most of the solvent. Subsequently, the mixture was placed into a hot vacuum oven kept at 120°C to remove the residual solvent. In the next stage, the stoichiometric amount of hot DDS was added to the mixture with a fierce stir to dissolve DDS completely. Next, the mixture was cast into a preheated mould treated with a release agent. Before the beginning of the curing reaction, the mould was placed in a hot vacuum oven maintained at 120°C to degass for 30min. At last, the mould was maintained at 120°C for 24h and additional 2h at 180°C (post-curing). As a control, another mould was cured at 180°C for 3h directly.

2.2.2 Preparation of epoxy resin, PES/epoxy blend, nanocomposites

The preparing method of hybrid nanocomposites was used to synthesize these samples by omitting the process of blending PES, adding organoclay or both of them.

2.3 Morphology characterization

2.3.1. X-ray diffraction (XRD)

XRD was performed on a D/max-γB diffractometer with a Cu Kα radiation ($\lambda=0.154\text{nm}$) produced by Rigaku Corporation. The acceleration voltage and current were 40kV and 20mA, respectively. The speed of scanning and the step length were 0.6°min^{-1} and 0.006° , respectively. The 2θ was ranging from 0.6° to 10° .

2.3.2 .Optical microscope (OM) observation

The uncured mixtures and cured specimens were placed between two glass slides under a Microscope (Keyence VH-Z500R) to observe the dispersion of organoclay in the matrix.

2.3.3. Scanning electron microscope (SEM) observation

The specimens were divided into two groups whose compositions were identical. One group was fractured and placed into methylene chloride and stirred vigorously for more than 48h to rinse out PES. Then the rinsed specimens were coated with a layer of gold around 200Å thick before the observation. The other group was fractured according to the method of the single-edge-notch three-point-bending (SEN-3PB) test. Next the fractured specimens were directly coated with a layer of gold for the observation. Finally, the specimens were observed by a scanning electron microscope (Philips XL-30).

2.3.4. Transmission electron microscope (TEM) analysis

A JOEL JEM-2100F transmission electron microscope was used at an accelerating voltage of 200kV to observe the thin specimens of 50nm to 60nm thickness microtomed by a microtome (LKB Bromma 2088 ultratome V) at room temperature. Before the observation of PES micro-domains in the matrices, several specimens were stained with OsO_4 for 72h.

2.4. Thermal properties test

2.4.1. Dynamic mechanical thermal analysis (DMTA)

DMTA properties of all the samples were measured by a DMA Q800 analyzer produced by TA Instruments Corporation at a fixed frequency of 1Hz and a heating rate of $3^\circ\text{C}/\text{min}$. Liquid nitrogen was used to control the system temperature. The tests were conducted under dual cantilever mode for the samples of size 60mmX6mmX3mm.

2.4.2. Thermogravimetric analysis

The thermal stability of the neat epoxy resin, PES/epoxy blend and hybrid nanocomposites were

measured by NETZSCH STA 449C thermal analyzer from room temperature to 1000 °C at a heating rate of 20 °C/min in nitrogen atmosphere.

2.5 Mechanical properties

2.5.1 Uniaxial compression test

Uniaxial compression test was used to investigate the ductility of the neat cured epoxy resin and the PES-modified epoxy resin according to ASTM D695-08. The specimen sizes are 5 by 5 by 10mm and the specimens are in the form of prism. The pristine samples were carefully mechanically cut and polished to produce perfectly parallel end surfaces and smooth surfaces. A screw-driven Instron (Model 5569) was used to carry out the test at a crosshead speed of 0.5mm min⁻¹.

2.5.2 Fracture toughness assessment

The fracture toughness of all the cured samples was measured from the critical stress intensity factor (K_{IC}) in the single-edge notched three-point bending (SEN-3PB) test based on ASTM D5045-99. The dimension of each sample was 70mm(L)X10mm(W)X5mm(B). The span for the fractured test was 40mm(S). The crack was prepared by machining a sharp notch on one surface of each sample and then inserting a fresh razor blade into the notch and tapping to make a sufficiently sharp natural crack. A screw-driven Instron machine (Instron 5569) was used at a crosshead speed of 0.5mm/min. At least five specimens of each composition were measured in this test.

3. Results and Discussions

DMTA measurement was first used to investigate the phase morphology in these samples. As shown in Fig. 1, there are only single glass transition peaks in all the DMTA curves. The result means that phase decomposition did not occur and PES-rich phase and epoxy-rich phase were absent in the PES modified samples.

SEM technology was used to further observe the phase morphology in the PES modified samples. In Fig.2, the SEM images from (a-1) to (a-6) and from (b-1) to (b-6) are for the fractured cross-sections of PES modified samples before being rinsed by methylene chloride and after being rinsed by methylene chloride for 48h, respectively. The fractured surfaces of these samples did not change even though they were rinsed sufficiently to get rid of PES. For the PES/epoxy blends, their fractured

surfaces were as smooth as the fractured surface of the cured neat epoxy resin. This result indicates that phase separation has been suppressed greatly, which accords with the prediction in the phase diagram in reference[9]. Although the incorporation of organoclay into the organoclay/poly(ether imide)/epoxy hybrid nanocomposite has been observed facilitating the formation of co-continuous structure [10] by improving the phase shape relaxation time [11] and the cloud points which were induced by the increase in the viscosity of the reaction mixture, the content of PES and organoclay in our reaction mixture is not high enough to markedly change the relaxation time and cloud points to ensure the occurrence of phase separation and coarsening. On balance, there are only single-phase structures in all the PES-modified samples. It should also be noted that the initial curing temperature of 180 °C was not high enough to enable phase decomposition too(compare Fig.2(a-4), Fig.2(a-5) and Fig.2(a-6) with Fig.2(b-4), Fig.2(b-5) and Fig.2(b-6), respectively). Therefore, the morphologies of the matrices in all the samples can be kept homogenous in this experiment.

However, it is clear from Fig.1 that T_g s of the PES modified samples cured at 120 °C are ca. 10 °C higher than the samples with same compositions cured at 180 °C. There could be some differences in the microstructure of these samples.

In the following, TEM method was used to further observe the phase microstructure of the PES/epoxy blends which were the matrices of hybrid nanocomposites and neat epoxy resin which was the matrices of nanocomposites. Before the observation the cured epoxy resin and PES/epoxy blends were stained with OsO₄ for 72h. As shown in Fig.3, there is a large discrepancy between the micrograph of PES/epoxy sample cured at 120 °C and that of PES/epoxy sample cured at 180 °C. The dark regions are the stained epoxy matrix, while the white regions are the PES micro-domains (see Fig. 3(a)). The PES micro-domains ca. 50nm in diameter interconnecting with each other are evenly distributed throughout the epoxy matrix. They seem to get entangled with epoxy network to form a semi-IPN structure making the whole image show a rough pattern. However, these interconnected spherical micro-domains vanish in the PES/epoxy blend cured at 180 °C (shown in Fig.3(b)). The micro-domains are far finer than those

of the blend cured at 120 °C. The whole image indicates a smooth structure which is similar to that of the neat cured epoxy resin(Fig.3(c)). These different micro-structures may influence the thermal performances and mechanical properties of the hybrid nanocomposites.

Organoclay has been used to toughen epoxy resins since 1990s. It has been widely accepted that the morphology of organoclay layers significantly influenced the properties of the nanocomposites. As two typical morphologies of organoclay layers, intercalated structure and exfoliated structure are often found in the cured epoxy matrix. In this study, XRD was used to characterize the morphology of organoclay in the nanocomposites and hybrid nanocomposites (presented in Fig.4). According to the patterns, no peaks are observed in all the samples except the pristine clay and neat organoclay whose peak values are ca. 5.5° (d-spacing 1.60nm) and 3.5° (d-spacing 2.52nm), respectively. The result indicates the intercalated structure is absent in all the nanocomposites and hybrid nanocomposites. Since the 2θ is ranging from 0.6° to 10°, all the d-spacings of the dispersed organoclay are larger than 12nm in accordance with the Bragg's relation: $\lambda = 2d \sin \theta$, where λ is the wavelength of the X-ray radiation, d is the spacing between the individual clay layers, θ is the measured diffraction angle. There is no van der Waals force between the individual layers of organoclay when the spacing between the layers exceeds 8nm. Therefore, the result means that exfoliated structures formed. Furthermore, it is apparent that the incorporation of PES into the nanocomposites did not change the final morphology of dispersion of organoclay. Moreover, the increase in the content of organoclay and the curing temperature in the reaction system did not affect the formation of exfoliated structure too.

Although the absence of diffraction peaks of 2θ in the range of 1.0° to 10° usually suggests the clay structures are mainly exfoliated, it is still quite difficult to differentiate ordered exfoliation from full exfoliation on the X-ray diffraction spectra. Consequently, TEM was used to further observe the morphology of organoclay in the nanocomposites and hybrid nanocomposite. A series of typical TEM images presented in Fig.5 show that organoclay has mainly ordered exfoliated structure in the hybrid nanocomposites with 1wt% organoclay(cured at

120°C). In addition, all the d-spacings are more than 12nm (from Fig.5(a) to Fig.5(d)) and part of the outer layers are fully exfoliated into the matrix(see Fig.5(a) and Fig.5(b)). The TEM images of the hybrid nanocomposite with 1wt% organoclay(cured at 180°C), the hybrid nanocomposites with 3wt% organoclay(cured at 120°C and 180°C, respectively) and the nanocomposites(cured at 120°C and 180°C, respectively) which are not demonstrated here show the same morphologies of organoclay as these pictures. The results accord with the results obtained from the XRD graph above. As a solvent for PES, methylene chloride also acted as a good dispersing agent for the exfoliation of organoclay.

In order to investigate the effect of the morphology of the matrices and organoclay on the thermal properties of the hybrid nanocomposites, DMTA measurement was done. All the T_gs(Tan δ peaks in Fig.1) listed in Table 1 are divided into three groups. There is a decreased trend in T_gs with the increase in the content of organoclay in each group. The drop of the T_gs can be first interpreted as the reaction of excess monoamine intercalating agents (octadecylamine which was used to organically treat the pristine clay) with the epoxy monomers. Moreover, the quaternary ammonium ions in the reaction mixtures underwent thermal dissociation and generated primary amines which could react with the epoxy resin. Furthermore, the hydrocarbon chain of octadecylamine began to degrade when the curing temperature rose to 180°C. These three aspects plasticized the epoxy networks leading to the shift of T_gs from high temperature to low temperature. It is interesting that the T_g of each sample in group one shifted ca. 10°C higher than that of the sample with the same content of organoclay in group two and group three. It can be concluded combined with the TEM result that it is the semi-IPN structure that gives rise to the increased T_gs of the samples in group one. The absence of the semi-IPN structure in the samples of group two(cured at 180°C) leads to almost identical T_gs compared with the corresponding samples without the incorporation of PES in group three. The results also indicate that the PES modification has little effect on the T_gs of the samples without forming semi-IPN structure.

The thermal stability of the hybrid nanocomposites were studied by thermogravimetric

analysis(TGA). The TGA curves shown in Fig.6 demonstrate the thermal stability of the samples cured at 120 °C. In Fig.6, it is obvious that the degradation began at 396 °C for the neat epoxy resin, while the onset were at 400 °C for PES/epoxy blend, 401 °C for the hybrid nanocomposite with 1wt% organoclay and 404 °C for the hybrid nanocomposite with 3wt% organoclay, respectively. It can be seen from the result that the thermal stability of samples increases with the incorporation of PES and the increase in the content of organoclay even though methylene chloride used as the solvent in the experiment can lower the thermal degradation temperature of the samples.

The fracture toughness of the samples was performed according to ASTM5045-99. Their K_{IC} values are presented in Table 2. It can be seen firstly that the neat epoxy resin owns the lowest value, while the nanocomposites cured at 120 °C are the highest two K_{IC} values. Besides, the K_{IC} values of the PES modified samples cured at 120 °C are higher than those of the samples with the same composition cured at 180 °C. Furthermore, the K_{IC} values of neat epoxy resin and nanocomposites increase after being modified by PES. Moreover, the K_{IC} values of neat epoxy resin and PES/epoxy blends increase after being reinforced by organoclay. Finally, the K_{IC} value of the nanocomposite with 3wt% organoclay is markedly higher than that of the nanocomposite with 1wt% organoclay, while there is only a slight increase in the K_{IC} value of the hybrid nanocomposite with 3wt% organoclay cured at 180 °C compared with that of the hybrid nanocomposite with 1wt% organoclay cured at 180 °C and a drop in K_{IC} value can be seen in the hybrid nanocomposite with 3wt% organoclay cured at 120 °C in comparison to that of the hybrid nanocomposite with 1wt% organoclay cured at 180 °C.

uniaxial compression test was performed to the investigate the ductility of the matrices in the nanocomposites and hybrid nanocomposites. Fig.7 shows that the yield stress decreases and the final breaking strength and the final breaking strain increases with the incorporation of PES. For the PES/epoxy blend cured at 180 °C, the yield stress drops makedly. It indicates that the intrinsic ductility of the neat epoxy resin were improved by the

incorporation of PES. Although the yield stress only decreases slightly for the PES/epoxy blend cured at 120 °C, it has the largest final breaking strength and the final breaking strain. It can be concluded from the TEM micrograph shown in Fig.5 that the formation of semi-IPN structure in the blend may lead to the slight decrease in the yield stress and the largest final breaking strength and the final breaking strain.

SEM micrographs shown in Fig. 8 further reveal the higher ductility of matrices of the hybrid nanocomposites compared with the nanocomposite. More deep characteristic tail structures and river markings around organoclay agglomerates formed in the hybrid nanocomposites(shown in Fig. 8(a) and Fig. 8(b)) by the resistance of the organoclay agglomerates to the crack propagation compared with the control without PES in Fig. 8(c). The result indicates that the matrix of the hybrid nanocomposite cured at 120 °C possesses the highest toughenability due to the formation of semi-IPN structure. Although the improved ductility of the matrix of the hybrid nanocomposite cured at 180 °C can be easily found compared with the relatively smooth surface of the nanocomposite, its toughenability was still much lower than that of the hybrid nanocomposite cured at 120 °C.

Therefore, the incorporation of PES into the epoxy resin and the nanocomposites can enhance the ductility of their matrices and further improve their toughenability and K_{IC} values. The existence of semi-IPN structure in the PES/epoxy blend and hybrid nanocomposite cured at 120 °C leads to the higher K_{IC} values compare with those cured at 180 °C.

SEM technology and TEM technology were then used to observe the fracture behavior of the organoclay agglomerates in the SEN-3PB fractured samples. The characteristic tail structures and river markings can be clearly seen around the orderedly exfoliated organoclay agglomerates in the hybrid nanocomposite with 1wt% organoclay(shown in Fig.9(a) and Fig.9(b)), while the surface of the fractured cross-section gets more rough for the hybrid nanocomposite with 3wt% organoclay (shown in Fig.9(c)). More characteristic tails interconnecting with each other appear (shown in Fig.9(d)).

Therefore, the highest fracture toughness of the hybrid nanocomposite with 1wt% organoclay cured

at 120 °C is due to the improved ductility of the matrix by the formation of semi-IPN structure and the resistance of organoclay agglomerates to the crack propagation by forming characteristic tails and river markings.

References

- [1] M. Callaghan "Use of resin composites for cryogenic takage". Cryogenics, Vol. 31, pp 282-287, 1991.
- [2] K. Yamanaka, T. Inoue "Structure development in epoxy resin modified with poly(ether sulphone)". Polymer, Vol. 30, pp 662-667, 1989.
- [3] A. Kinloch, A. Taylor "Mechanical and fracture properties of epoxy-inorganic micro- and nanocomposites". Journal of Materials Science letters, Vol. 22, pp 1439-1441, 2003.
- [4] T. Inoue "Reaction-induced phase decomposition in polymer blends". Prog Polym Sci, Vol.20, pp 119-153, 1995.
- [5] H. Kishi, Y. Shi, J. Huang, A. Yee "Shear ductility and toughenability study of highly cross-linked epoxy-polyethersulphone". Journal of Materials Science, Vol. 32, pp 761-771, 1997.
- [6] J. Lee, A. Yee "Micro-mechanical deformation mechanisms in the fracture of hybrid-particulate composites based on glass beads, rubber and epoxies". Polymer Engineering and Science, Vol. 40, pp 2457-2470, 2000.
- [7] J. Park, S. Jana "The relationship between nano- and micro-structures and mechanical properties in PMMA-epoxy-nanoclay composites". Polymer, Vol. 44, pp 2091-2100, 2003.
- [8] D. Ratna, O. Becker, R. Krishnamurthy, G. Simon, R. Varley "Nanocomposites based on a combination of epoxy resin, hyperbranched epoxy and a layered silicate". Polymer, Vol.44, pp 7449-7457, 2003.
- [9] K. Mimura, H. Ito, H. Fujioka "Improvement of thermal and mechanical properties by control of morphologies in PES-modified epoxy resins". Polymer, Vol. 41, pp 4451-4459, 2000.
- [10] M. Peng, H. Li, L. Wu, Y. Chen, Q. Zheng, W. Gu "Organically modified layered-silicates facilitate the formation of interconnected structure in the reaction-induced phase separation of epoxy/thermoplastic hybrid nanocomposite". Polymer, Vol. 46, pp 7612-7623, 2005.
- [11] E. Siggia "Late Stages of Spinoidal Decomposition in Binary Mixtures". Phy Rev A, Vol. 20, pp 595-605 1979.

Tables, Diagrams and Figures

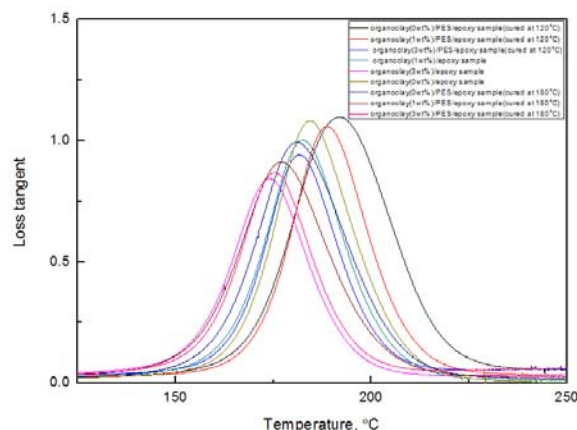


Fig.1 DMTA curves of Loss tangent vs. temperature for the samples consisted of the neat epoxy resin, PES/epoxy blend, nanocomposites and hybrid nanocomposites

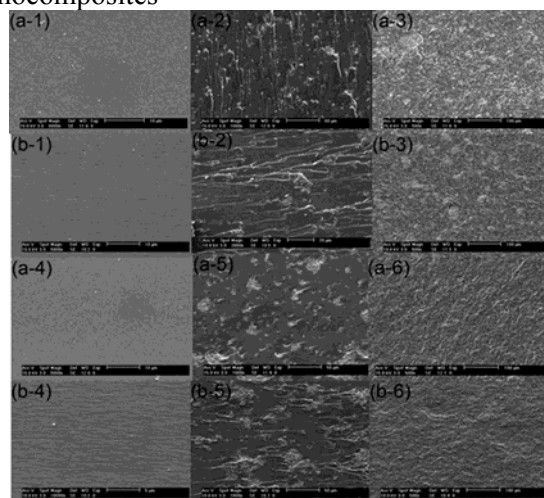


Fig.2 SEM images for the fractured cross-sections of the samples after being rinsed (from (a-1) to (a-6)) and before being rinsed (from (b-1) to (b-6)) ((a-1),(b-1): organoclay(0wt%)/PES/epoxy samples cured at 120 °C ; (a-2),(b-2): organoclay(1wt%)/PES/epoxy samples cured at 120 °C ; (a-3),(b-3) : organoclay(3wt%)/PES/epoxy samples cured at 120 °C ; (a-4),(b-4): organoclay(0wt%)/PES/epoxy samples cured at 180 °C ; (a-5),(b-5): organoclay(1wt%)/PES/epoxy samples cured at 180 °C ; (a-6),(b-6) : organoclay(3wt%)/PES/epoxy samples cured at 180 °C). All the samples were sufficiently rinsed with methylene chloride.

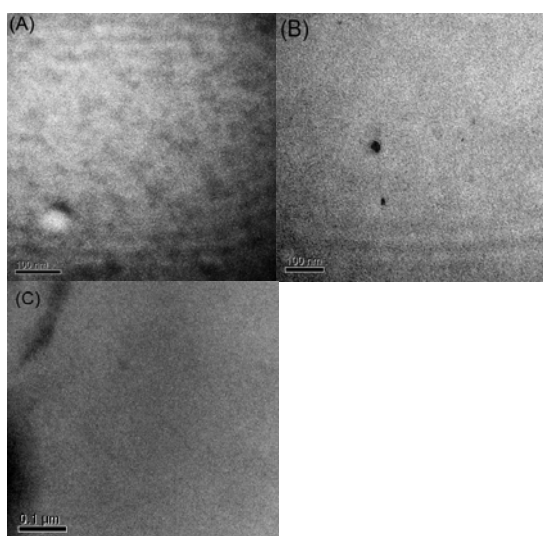


Fig.3 TEM micrographs of PES/epoxy blends and neat epoxy resin with homogeneous morphology: (A) PES/epoxy blends (cured at 120°C); (B) PES/epoxy blends(cured at 180°C) ; (C) neat epoxy resin (cured at 120°C).

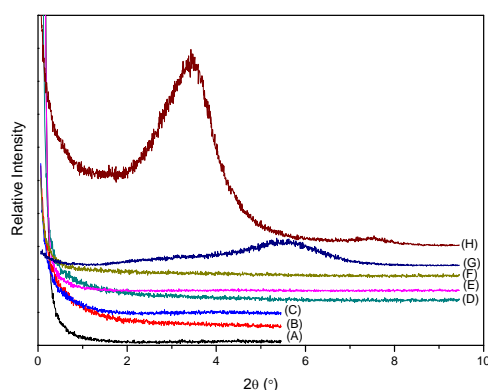


Fig.4 XRD patterns of pristine clay, organoclay, nanocomposites and hybrid nanocomposites: (A) organoclay(1wt%)/PES/epoxy sample cured at 120 °C ; (B)organoclay(3wt%)/PES/epoxy sample cured at 120 °C ; (C) organoclay(1wt%)/PES/epoxy sample cured at 180 °C ; (D)organoclay(3wt%)/PES/epoxy sample cured at 180 °C ; (E) organoclay(1wt%)/epoxy sample; (F)organoclay(3wt%)/epoxy sample; (G) pristine clay; (H)organoclay.

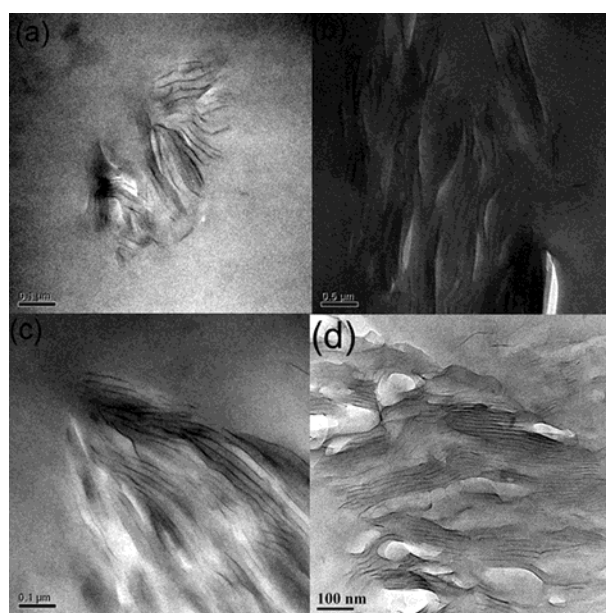


Fig.5 TEM images of the morphologies of organoclay in the hybrid nanocomposites with 1wt% organoclay((a),(b): small agglomerates of organoclay; (c)(d): large agglomerates of organoclay).

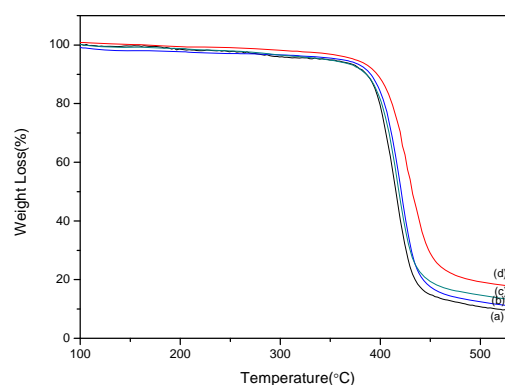


Fig.6 TGA thermograms of the pure epoxy resin, PES/epoxy blend and hybrid nanocomposites: (a)neat epoxy sample; (b)PES/epoxy sample; (c)organoclay(1wt%)/PES/epoxy sample; (d)organoclay(3wt%)/PES/epoxy sample. All the samples were cured at 120°C.

Table 1 Tgs of three groups of samples

	0wt% organoclay	1 wt% organoclay	3 wt% organoclay
group 1	192°C	189°C	181°C
group 2	181°C	177°C	175°C
group 3	185°C	182°C	174°C

Note: group 1: samples with PES cured at 120°C; group 2: samples with PES cured at 180°C; samples without PES cured at 120°C.

Table 2 Fracture toughness of the neat epoxy resin, PES/epoxy blends, nanocomposites and hybrid nanocomposites at different curing temperatures

(cured at 120°C)	neat epoxy	organoclay(1wt%)/epoxy	organoclay(3wt%)/epoxy
K_{IC} (MPa m ^{1/2})	0.58±0.11	0.73±0.05	0.81±0.06
(cured at 180°C)	PES/epoxy	organoclay(1wt%)/PES/epoxy	organoclay(3wt%)/PES/epoxy
K_{IC} (MPa m ^{1/2})	0.73±0.03	0.78±0.02	0.80±0.02
(cured at 120°C)	PES/epoxy	organoclay(1wt%)/PES/epoxy	organoclay(3wt%)/PES/epoxy
K_{IC} (MPa m ^{1/2})	0.77±0.10	1.15±0.10	0.93±0.05

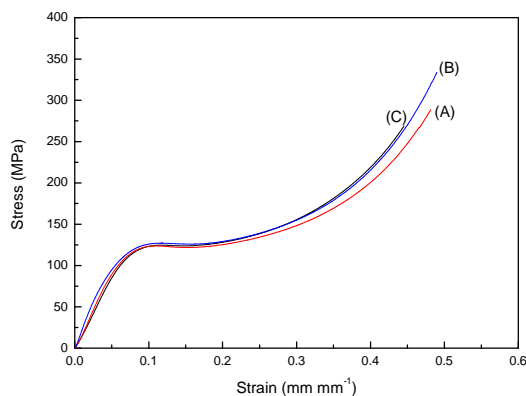


Fig.7 Uniaxial compression test results: (A) PES/epoxy blend cured at 180 °C; (B) PES/epoxy blend cured at 120 °C; (C) neat epoxy resin.

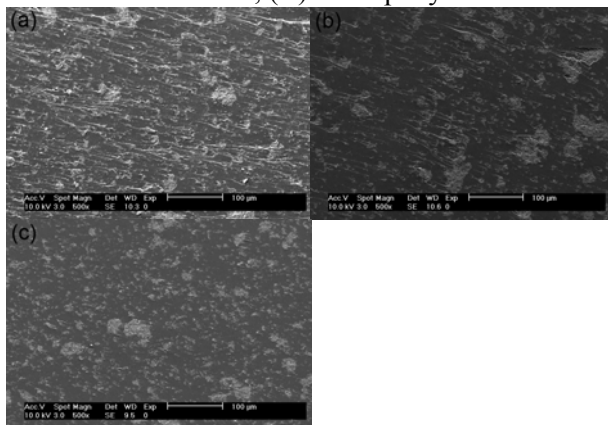


Fig.8. SEM micrographs of the fractured surfaces of the organoclay filled samples in SEN-3PB test: (a)organoclay(1wt%)/PES/epoxy sample cured at 120 °C ; (b)organoclay(1wt%)/PES/epoxy sample cured at 180°C; (c)organoclay(1wt)%/epoxy sample.

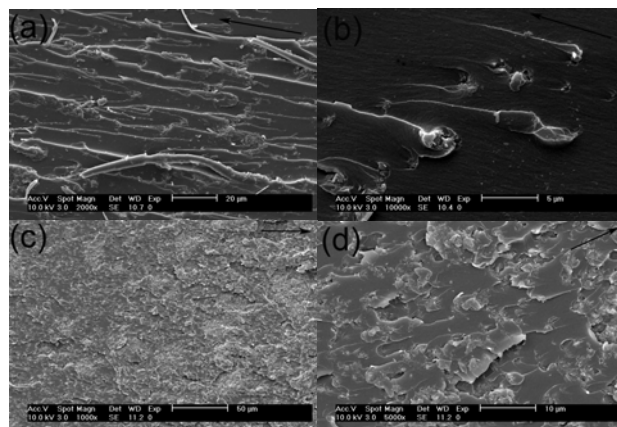


Fig. 9 SEM images of the fracture cross-sections of the hybrid nanocomposites: (a)River markings on the fracture cross-section of the hybrid nanocomposite with 1% organoclay; (b)Characteristic tail structures on the fracture cross-section of the hybrid nanocomposite with 1wt% organoclay; (c)The rough surface of the fracture cross-section of the hybrid nanocomposite with 3wt% organoclay; (d) Characteristic tail structures and river markings on the fracture cross-section of the hybrid nanocomposite with 3wt% organoclay. The arrows in the images indicate the direction of crack propagation.